JOURNAL OF THE CHINESE INSTITUTE OF ENGINEERS
2021, VOL. 44, NO. 6, 553–561
https://doi.org/10.1080/02533839.2021.1936646

Negative moment region flexural strengthening system of RC T-beams with half-embedded NSM FRP rods: a parametric analytical approach

Yanuar Haryanto[a,b], Hsuan-Teh Hu[a,c], Ay Lie Han[d], Fu-Pei Hsiao[a,e], Charng-Jen Teng[a], Banu Ardi Hidayat[a,d] and Nanang Gunawan Wariyatno[b,d]

[a]Department of Civil Engineering, National Cheng Kung University, Tainan, Taiwan (R.O.C); [b]Department of Civil Engineering, Jenderal Soedirman University, Purbalingga, Indonesia; [c]Department of Civil and Disaster Prevention Engineering, National United University, Miaoli, Taiwan (R.O.C); [d]Department of Civil Engineering, Diponegoro University, Semarang, Indonesia; [e]National Center for Research on Earthquake Engineering, Taipei, Taiwan (R.O.C)

ABSTRACT

Fiber Reinforced Polymer (FRP) rods are considered to be the most effective in retrofitting to increase the strength of reinforced concrete (RC) structures through Near-Surface Mounted (NSM) technique. There are, however, frequent cases encountered by engineers where the embedment depth mandated by ACI 440.2 R-08 code is not achievable in the field implementation. It has also been discovered that it is more challenging to strengthen the negative moment region of concrete members in comparison with the positive region. This research was conducted to determine the behavior of RC T-beams strengthened in the negative moment region using half-embedded NSM FRP rods. The findings were associated with the Modified Compression Field Theory (MCFT) which was applied in the analytical models. The model proposed was validated through a comparison with previous experimental study that showed half-embedded NSM FRP was effective as another method in comparison with the conventional soffit strengthening systems in retrofitting RC T-beams in the negative moment region, and good agreement was obtained. After that, a parametric analysis was initiated to determine the influence of FRP rod diameters, the compressive strength of concretes, the ratio of steel reinforcement as well as the materials used for the FRP on the flexural behavior of strengthened beams.

ARTICLE HISTORY
Received 31 October 2020
Accepted 24 May 2021

KEYWORDS
An analytical study; flexural strengthening; fiber reinforced polymer; negative moment region; half-embedded

1. Introduction

The worry created by the numbers of human beings lost and the financial casualties associated with inadequacy in structural performance observed as buildings age and degrade have led to an awareness of the urgent need to retrofit to increase the strength of reinforced concrete (RC) structures. Some of the other reasons to retrofit the strength of RC structures include concrete degradation, corroding bars, observable damage, aging concrete structures, unpredictable loads exposure as observed in strong earthquakes and shock loads, improvement in design standard codes, errors and mistakes made in the process of design and construction, and variations in the usage of a structure (Nordin and Täljsten 2006). It is, however, possible to resolve all these comprehensive structural deficiency classifications through the use of Fiber Reinforced Polymer (FRP) composites as a feasible strengthening method for RC members (Lin et al. 2014).

FRP was produced through the embedment of continuous fibers in a polymeric resin matrix as a material to ensure the enhancement of RC structures' serviceability and load-carrying capacity. It was widely accepted by engineers and applied as a substitute for other methods of strengthening, especially due to its several advantages such as the reduction in structure's dead load, significant strength to weight ratio, resistance to corrosion, and durability which leads to its application in construction projects where traditional materials are not allowed to be used (Bakis et al. 2002; Hollaway and Teng 2008). However, FRP has several drawbacks such as the lack of ductility (Peled 2007; Zhang et al. 2019) and quick softening at high temperatures (Firmo, Correia, and Bisby 2015; Fayed, Basha, and Hamoda 2019) but its application has been reported to be one of the most cost-effective methods of strengthening (Grace et al. 1999). It was observed to have a better performance than steel plate, a popular traditional method of strengthening, which corrodes after exposure (Qeshta, Shafigh, and Jumaat 2016), experiences detachment and has several challenges due to the steel plates' weight in beams with large span. Moreover, Raithby (1982) and MacDonald and Calder (1982) conducted exposure tests and found a significant amount of corrosion occurring at the interface of steel/epoxy, thereby, causing a reduction in the concrete's strength and local debonding.

Strengthening the negative moment region of concrete members has been reported to be more challenging compared to the positive region. Jumaat, Rahman, and Alam (2010) addressed some practical problems associated with strengthening the negative moment region of a continuous span, which

CONTACT Yanuar Haryanto yanuar_haryanto@yahoo.com Department of Civil Engineering, National Cheng Kung University, No. 1 University Road, Tainan 701, Taiwan (R.O.C)

This article has been corrected with minor changes. These changes do not impact the academic content of the article.

is considered a critical zone due to the presence of large moment and shear at the same location. Moreover, the presence of the columns at such locations prevents the application of the strengthening system over the web portion of the beam (Al-Khafaji and Salim 2020). An experimental investigation has been conducted by Sapulete (2018) to evaluate the half-embedded Near-Surface Mounted (NSM) FRP rods strengthening techniques in the negative moment region of RC T-beams due to the frequent cases requiring embedment depth mandated by ACI 440 (2008) code but not achievable by engineers in the field due to structural frames of buildings. The results showed the FRP rods mounted only for half the area of the rod increased the moment carrying capacity of the member by 30% but ductility did not significantly improve and no clear pattern was noticed in conventional steel after yielding. This means it is possible to practically apply half embedded rods under the condition that the bonding agent is applied to the rods using the method stated by the producer.

In order to continually expand the scope of the study conducted by Sapulete (2018), this research developed an analytical model to predict the flexural capacity of half-embedded NSM FRP rod-strengthened RC T-beams in the negative moment region based on Modified Compression Field Theory (MCTF) (Vecchio and Collins 1986) applied in a program, Response-2000, which is commonly known as R2K (Bentz 2000). This combination, however, offers users the opportunity to fully comprehend and investigate the responses of beams and columns of any shape and material under the influence of moment, shear, and axial loads. Comprehensive outcomes were obtained from the experiments but they were specific to the particular placement of strain gauges and Linear Variable Differential Transformers (LVDTs) despite the huge cost and time expended on the process. Meanwhile, Huang et al. (2019) demonstrated an accurate simulation of the mean shear strain of specimens using R2K. The same method was also applied by Lam and Lumantarna (2011) to model the force-deformation behavior of cracked reinforced concrete with fiber elements and all specimens with varying cross-sectional areas were predicted to have comparable moments of resistance. Furthermore, Metwally (2012) gauged the efficiency as well as the validity of the R2K software to predict the shear capacities of reinforced and pre-stressed concrete elements and found its predictions concerning failure shear to be characterized by an average observed-to-predicted shear ratio equaling 1.05 and a coefficient of variation equaling 12%. Suryanto, Morgan, and Han (2016) also supported the accuracy of R2K to predict the load-deflection behavior demonstrated by shear-critical concrete beams up to the peak load.

2. Development of the analytical model

2.1. Description of experimental program

The analytical evaluation results were validated through a comparison with an experimental study conducted by Sapulete (2018) to investigate the behavior of RC T-beams strengthened in the negative moment region with two 8 mm half-embedded NSM Carbon Fiber Reinforced Polymer (CFRP) rods (BS) along with unstrengthened specimen (BN). The beams were observed to have the ability to sustain an increment in one-point loading or three-point bending up to the moment the specimens experienced failure. The total length of the beam was recorded to be 2500 mm with the distance from a center to another found to be 2300 mm while the total height of the T-section was 300 mm with a web-width of 150 mm, flange-width of 600 mm, and the flange-depth of 100 mm as shown in Figure 1. The average cylindrical concrete compressive strength was 36.29 MPa and the specimens were made to consist of two 19 mm ribbed bars in tension zone with

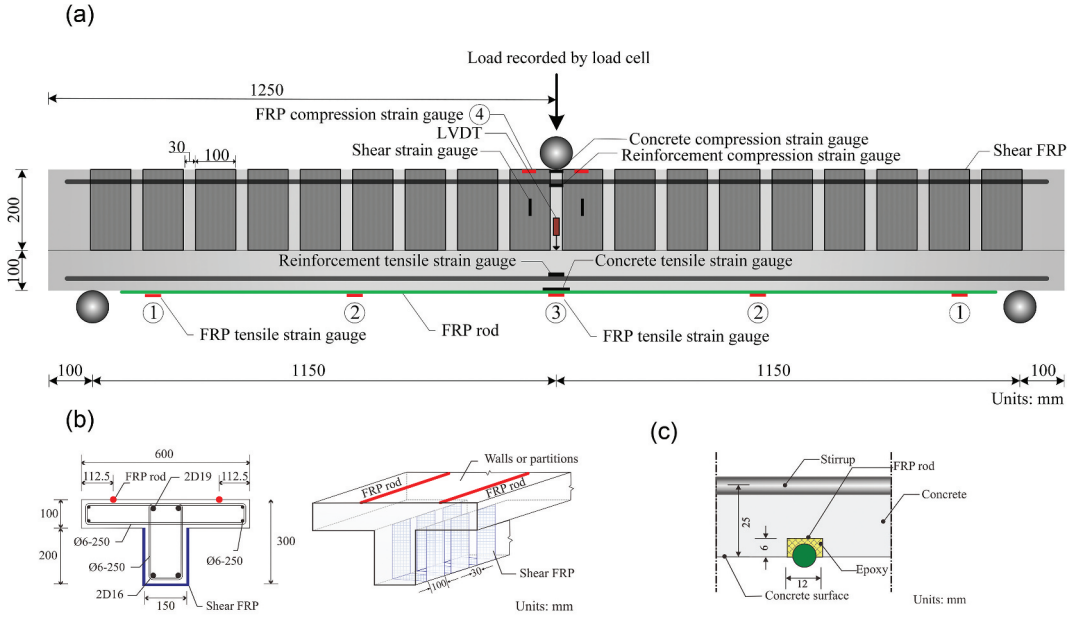

Figure 1. The details of the experimental setup and tested beams (Sapulete 2018). (a) Test setup; (b) Specimen details and FRP rods placement; (c) Half-embedded FRP rod detail.

407.90 MPa yield strength, two others with a diameter of 16 mm in compression zone with 402.90 MPa yield strength, and steel stirrups with 6 mm diameter having 371.04 MPa yield strength spaced 250 mm apart. The CFRP rod mechanical properties were obtained from PT. SIKA Indonesia with the modulus of elasticity recorded to be 148 GPa while the tensile strength was 3100 MPa. Meanwhile, the CFRP sheets had 225 GPa modulus of elasticity and 3850 MPa tensile strength, respectively, and were installed as shear strengthening along the entire span of the strengthened beam with 100 mm width and a 130 mm space apart.

By the application of the half-embedded NSM CFRP rods in the strengthened specimen (BS), an approximately 30% increase in ultimate load was observed compared to that of the control specimen as shown in Figure 2. It was also observed that the increases in the amount of mid-span deflection at ultimate load produced by CFRP strengthening was 5% compared to that of unstrengthened beam (BN). The first crack in the concrete's tension area for BN occurred at a loading level of 30% of the ultimate load, while the reinforced steel yielded at a loading level of 96% of the ultimate strength. Owing to significant shifting of the neutral axis toward the compression zone, the strains in the concrete fibers reached its failure-strain limit and the member failed due to the crushing of concrete in the compression area. The member underwent large deformations from the prolonged yielding of the steel bars, resulting in a post peak curve. The BS beam with the half-embedded CFRP rods behave almost identically. The concrete in tension cracked at levels of 32% of the ultimate load. The conventional steel bars yielded at around 100% of their controlling element's ultimate load (Sapulete 2018). Those outcomes show the effectiveness of half-embedded NSM FRP method as an alternative to conventional soffit strengthening systems to improve the flexural capacity of RC T-beams in the negative moment region.

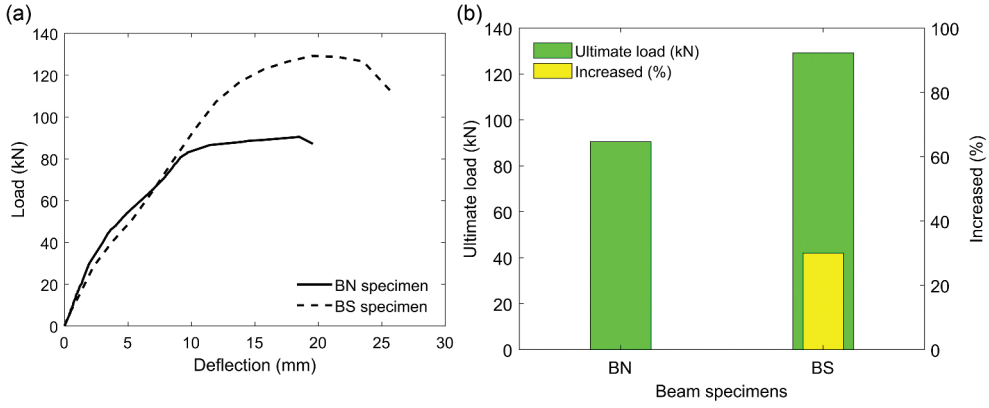

Figure 2. Summary of the experimental results. (a) Load–deflection curves of the tested beams; (b) Ultimate load of the tested beams.

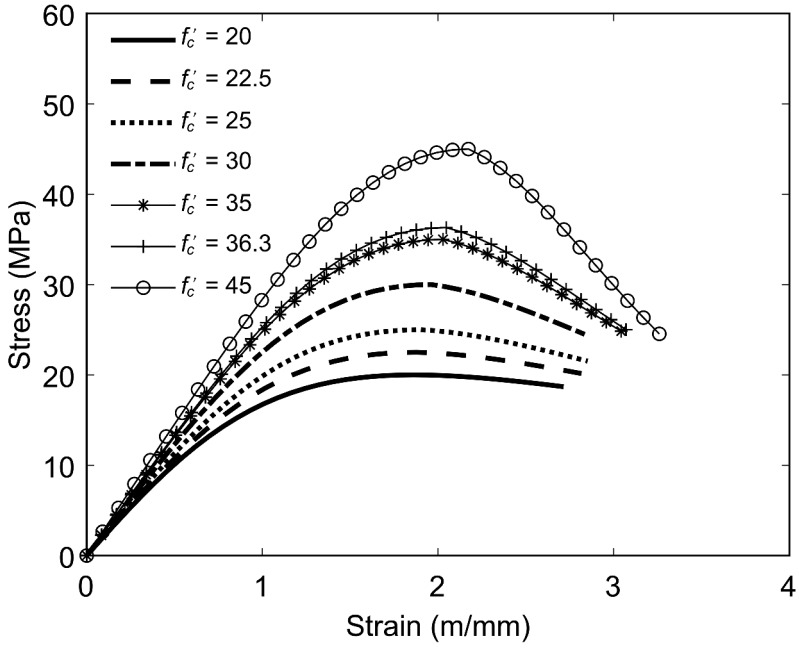

Figure 3. Compression stress versus strain curve for concrete.

2.2. Materials behavior

The non-linear characteristics of the concrete subjected to compression and stress-strain association were considered in the analytical models developed in R2K. The models expressed in Equations (1) to (3) were formulated by Popovics (1973) and slightly modified by Porasz (1989). Meanwhile, the stress versus strain curve for every concrete type is presented in Figure 3.

$$f_c = -\left(\frac{\varepsilon_c}{\varepsilon_{co}}\right) f_c' \frac{n}{n - 1 + (\varepsilon_c/\varepsilon_c\varepsilon_{co} - \varepsilon_{co})^{nk}}, \quad (1)$$

$$n = 0.8 + f_c'/17, \quad (2)$$

$$k = \begin{cases} 1.0 & \text{if } \frac{\varepsilon_c}{\varepsilon_{co}} < 1.0 \\ 0.67 + \frac{fc}{62} & \text{if } \frac{\varepsilon_c}{\varepsilon_{co}} > 1.0 \end{cases}, \quad (3)$$

where f_c is compressive stress of concrete (MPa) at a particular strain value (ε_c), fc' is compressive strength of concrete (MPa), ε_{co} is strain at peak compressive strength, n is curve fit parameter, and k is factor of loss in post-peak ductility for high-strength concrete. Equation (4) shows that R2K used the Bentz model for the non-linear material properties of concrete subjected to tension (f_t) (Bentz 2000).

$$f_t = 0.45(fc)^{0.4}, \quad (4)$$

The stress-strain response of steel reinforcement usually has three components which are (1) the initial linear-elastic response, (2) the yield plateau, and (3) the strain-hardening phase which is either linear or non-linear until rupture. The subsequent discussion on hysteretic behavior indicates the explanation of the backbone curve presented in models proposed by Seckin (1981) or Menegotto and Pinto (1973) through the monotonic stress–strain curve. Meanwhile, Equation (5) was used to compute the steel reinforcement stress, f_s, for both tension and compression.

$$f_s = \begin{cases} E_s\varepsilon_s & \text{for} \quad \varepsilon_s\, \varepsilon_y \\ f_y & \text{for} \quad \varepsilon_y\, \varepsilon_s \le \varepsilon_{sh} \\ f_u + (f_y - f_u)\left(\frac{\varepsilon_u - \varepsilon_s}{\varepsilon_u - \varepsilon_{sh}}\right) & \text{for} \quad \varepsilon_{sh}\, \varepsilon_s \le \varepsilon_u \\ 0 & \text{for} \quad \varepsilon_u\, \varepsilon_s \end{cases}, \quad (5)$$

The ε_s in the above equation denotes the strain ($\varepsilon_s = |\varepsilon_s|$), ε_y represents the yield strain, ε_{sh} is the initial strain at the beginning of strain hardening, ε_u is the ultimate strain, E_s is the elastic modulus, f_y is the yield strength, f_u is the ultimate strength, and P is the strain-hardening parameter. Moreover, the strain-hardening phases after the yield plateau have the potential to be linear (trilinear, $P = 1$) or nonlinear ($P = 4$). A perfectly elastic stress–strain curve was, however, generated by the trilinear option for the FRP rods used as the strengthening material. The stress–strain curve obtained for all type of steel reinforcement and FRP materials is presented in Figure 4 with the strain hardening modulus E_{sh}, if any, indicated in Equation (6) as follows:

$$E_{sh} = \left(\frac{f_u - f_y}{\varepsilon_u - \varepsilon_{sh}}\right), \quad (6)$$

3. Model validation

The developed analytical models were checked for validity and accuracy using two tested specimens, BN and BS beams, after which the data were compared with R2K predictions. The observed and predicted values of the load versus mid-span deflection at each loading are, however, presented in Figure 5 while the values for the predicted and experimentally observed values of ultimate attained load (P_u) are compared in Table 1. Moreover, the ratio of the experimentally observed value of P_u, denoted by $P_{u\text{-}Exp}$, to the predicted value of P_u, denoted by $P_{u\text{-}An}$ is also indicated in the Table.

Figure 5 shows the results of the experiment are comparable to the predicted responses with each beam found to initially show a linear-elastic followed by a transitional nonlinear and finally an almost linear response and this was observed to be continuous up to the peak load. This compatibility is significant due to its relation to the intricacy of the actual response caused by the promulgation of existing cracks and the development of new cracks. Consequently, a decline was discovered in the overall stiffness of the beam while the undesirable response was found near the peak with the ductility, particularly, found to likely be underestimated in the analytical predictions. Moreover, the normalized mean square error (NMSE) was recorded to be 0.007 based on the calculations from Table 1

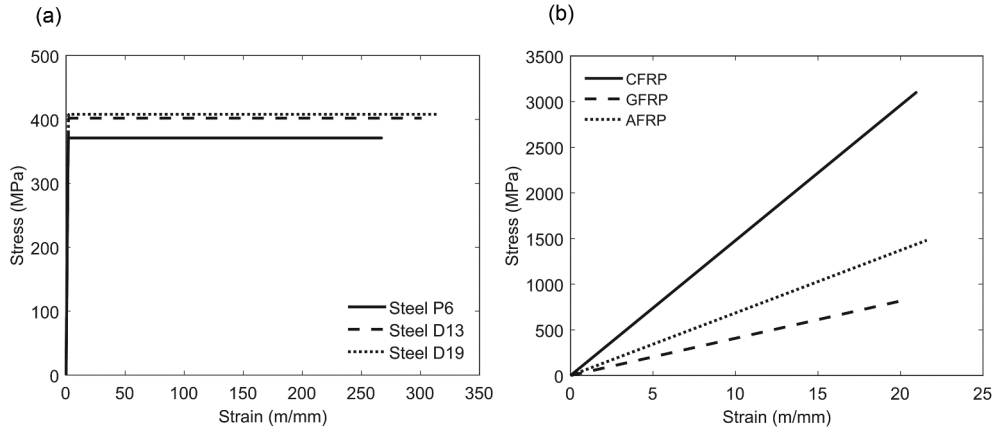

Figure 4. Tensile stress–strain curves. (a) Steel reinforcements; (b) FRP rods.

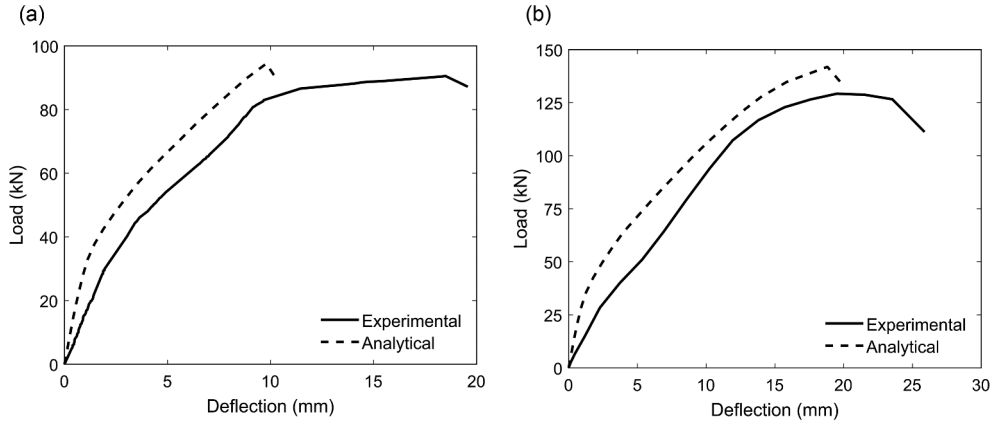

Figure 5. Comparison of experimental and predicted load-deflection curves. (a) BN beam; (b) BS beam.

Table 1. Verification of results from experimental and analytical models.

Specimens	P_u (kN)		Ratio
	Experimental	Analytical	$P_{u\text{-}Exp}/P_{u\text{-}An}$
BN	90.54	94.42	0.96
BS	129.23	141.88	0.91

Concrete compressive strength, f_c'=36.29 MPa
Steel reinforcement ratio, ρ = 1.4%
FRP rod diameter, d = 8 mm

and this means the situate is tolerable with consideration for the predicted flexural capacity, for example, as required from the design perspective. It should be noted that the developed analytical model did not take FRP sheets into consideration due to the limitations of the R2K program. However, it still can be used at this stage to determine the influence of FRP dimension, concrete compressive strength, the ratio of steel reinforcement, and FRP materials on the performance of strengthened RC beams through a design-oriented parametric study.

4. Parametric study

A design-oriented parametric study was conducted in this section through the development and analysis of 20 more models to determine the effect of FRP rods' diameters, compressive strength of concretes, ratio of steel reinforcement, as well as different types of the FRP rods on the flexural response and strength of the RC T-beams, which were strengthened in the negative moment region with NSM half-embedded FRP rods.

4.1. The effect of FRP rods diameter

Four models were used to determine changes in the response of the strengthened beams based on the adjustment of size or FRP rod diameter. One beam was not strengthened with FRP rods and used as the control specimen while the remaining specimens were strengthened using two half-embedded FRP rods with the diameters varied at 8, 10, and 12 mm to study the influence of change in dimension of FRP on the beams' behavior or response. The beams were all modeled to have a 30 MPa concrete compressive strength while designation for each as well as the summary and comparison between the predicted value of ultimate attained load (P_u) and the related value of mid-span deflection (δ_u) are presented in Table 2. Meanwhile, a graphical representation of the response curves to determine the correlation between the predicted load and mid-span deflection for all models is shown in Figure 6.

The information presented in Figure 6 and Table 2 shows the flexural strength and load-carrying capacity of the strengthened beams using the NSM technique with only half-embedded FRP were higher than the values recorded for the control beams (B-01), as predicted by the models. The specimen with 8 mm diameter FRP rods was significantly better, with 41.10% compared to the control in terms of the load-carrying

Table 2. Impact of FRP rod diameter variation.

Designation	FRP rod diameter (mm)	P_u (kN)	Percentage increase in P_u over the control beam	δ_u (mm)
B-01	–	94.01	–	10.27
B-02	8	132.65	41.10	17.16
B-03	10	134.96	43.57	15.95
B-04	12	137.72	46.50	15.02

Concrete compressive strength, f_c'=30 MPa
Steel reinforcement ratio, ρ = 1.4%

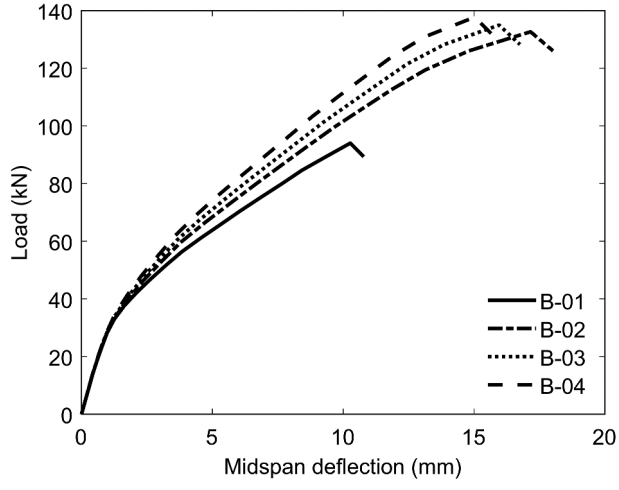

Figure 6. Influence of the dimension of FRP rod on beams' performance.

capacity (P_u), while an increment of 43.57% and 46.50% was observed in the flexural strength for specimens with 10 mm and 12 mm diameter of FRP rods, respectively, as shown in Table 2. This means there is a direct relationship with slight impact between the FRP rod diameter and the percentage increase in flexural capacity, given half-embedded rods. This effect is attributed to the fact that the increase in rod diameter causes an increment in the FRP rods' tensile force, thereby leading to a higher flexural capacity of the reinforced beam. It was also observed in Figure 6 and Table 2 that the mid-span deflection (δ_u) of P_u is comparable for all the strengthened beam models. This means the technique used led to the enhancement of beam models' strength while a nearly equivalent increased level of ductility was simultaneously maintained in the beams and this shows the effectiveness of using the method as an alternative.

4.2. The effect of concrete compressive strength

The effectiveness of strengthened RC beams is usually influenced by their compressive strength (f_c'). Therefore, six analytical models were developed with three used as control while the others were strengthened with two 8-mm-diameter NSM half-embedded FRP rods and modeled to have 25, 35, and 45 MPa compressive strength, respectively, and 1.4% steel reinforcement ratio as shown in Table 3. Meanwhile, the predicted curves obtained by plotting the load against the mid-span displacement for each developed model are presented in Figure 7. The predicted values of the ultimate attained load (P_u) and related values of mid-span deflection (δ_u) are also compared in Table 3.

Table 3 and Figure 7 show the insignificant impact of the compressive strength on the performance delivered by the control beam specimen and this was observed to be mainly due to the significant effect of the reinforcement steel strength on the flexural strength which is reflected through under-reinforced beam specimens. Moreover, the response and load-carrying capacity of strengthened beams were moderately affected by the compressive strength with their load-carrying capacity found to be higher than the control specimen. This is evident in the 35.51% recorded for specimen B-08 (f'_c 25 MPa), 48.50% for B-09 (f'_c 35 MPa), and 57.25% for specimen B-10 (f'_c 45 MPa). These numbers all refer to % of improvement over the control beam. This is likely due to the increment in the value of f_c' leading to higher tensile strength (f_t) for the concrete which ultimately affects the maximum local bond stress as well as the bond-slip behavior shown by the strengthening material, FRP rods in this case, and the concrete surfaces attached.

Table 3. Impact of varying the compressive strength of concrete.

Designation	f_c' (MPa)	P_u (kN)	Percentage increase in P_u over control beam	δ_u (mm)
B-05	25	93.79	–	10.90
B-06	35	94.38	–	9.89
B-07	45	95.58	–	9.31
B-08	25	127.09	35.51	16.59
B-09	35	140.15	48.50	18.44
B-10	45	150.29	57.25	21.51

Steel reinforcement ratio, ρ = 1.4%
FRP rod diameter, d = 8 mm

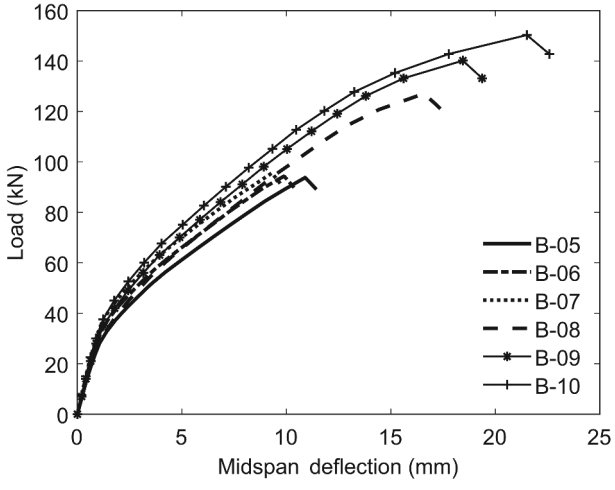

Figure 7. Influence of compressive strength on beams' performance.

4.3. The effect of steel reinforcement ratio

This study also explored how the performance of strengthened RC beams is affected by the steel reinforcement ratio (ρ) through the development of 6 analytical models out of which 3 were used as control while the remainder were strengthened using two half-embedded 8-mm-diameter NSM FRP rods. Steel flexural bars with three different areas including 2D19-mm, 3D19-mm, and 4D19-mm with ρ values of 1.4%, 2.1%, and 2.9% respectively were used in the model while the compressive strength was 20 MPa as shown in Table 4. Moreover, the predictions of the curves obtained by plotting the load against the mid-span deflection for each model are shown and compared in Figure 8 and the under-reinforced beams with a reinforcement ratio of 1.4% were observed to have a high percentage increase in ultimate load-carrying capacity by being 28.28% higher than the control while over-reinforced specimens with higher reinforcement ratios of 2.1% and 2.9% had low percentage increment of only 2.01% and 2.34%, respectively. Therefore, the transition from under-reinforcement to over-reinforcement leads to a higher steel reinforcement ratio and consequently greater reduction in the percentage increment in flexural strength of specimens strengthened using half-embedded NSM FRP rods. This means that as a strengthening material, the use of half-embedded NSM FRP rods has good effectiveness to retrofit the under-reinforced beam members.

Table 4. Impact of different values of steel reinforcement ratio.

Designation	ρ (%)	P_u (kN)	Percentage increase in P_u over control beam	δ_u (mm)
B-11	1.4	93.34	–	11.70
B-12	2.1	121.61	–	12.83
B-13	2.9	126.13	–	10.70
B-14	1.4	119.74	28.28	15.46
B-15	2.1	124.06	2.01	12.06
B-16	2.9	129.08	2.34	10.43

Concrete compressive strength, f_c'=20 MPa
FRP rod diameter, d = 8 mm

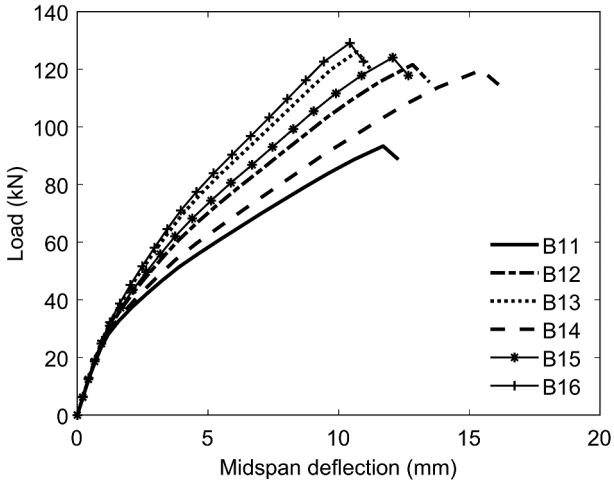

Figure 8. Influence of steel reinforcement ratio on the beams' performance.

Table 5. FRP materials attributes.

FRP material	Ultimate tensile strength (MPa)	Ultimate strain (%)	Elastic modulus (GPa)
CFRP*	3100	2.1	148.0
GFRP**	825	2.0	40.8
AFRP**	1480	2.1	68.6

*Sapulete (2018).
**Panahi and Izadinia (2018).

4.4. The effect of FRP material

The effect of the type of FRP materials on RC beams with half-embedded FRP rods flexural behavior was determined by developing and analyzing four analytical models with one used as control while the others were strengthened using two 8-mm-diameter Carbon Fiber Reinforced Polymer (CFRP), Glass Fiber Reinforced Polymer (GFRP), and Aramid Fiber Reinforced Polymer (AFRP) rods with 22.5 MPa compressive strength and 1.4% steel reinforcement ratio as shown in Table 5. Moreover, the designation of the beams, as well as the results anticipated for P_u and δ_u, are summarized in Figure 9 and Table 6.

Table 6 and Figure 9 show an increment in the values of the load-carrying capacity predicted for the strengthening of the

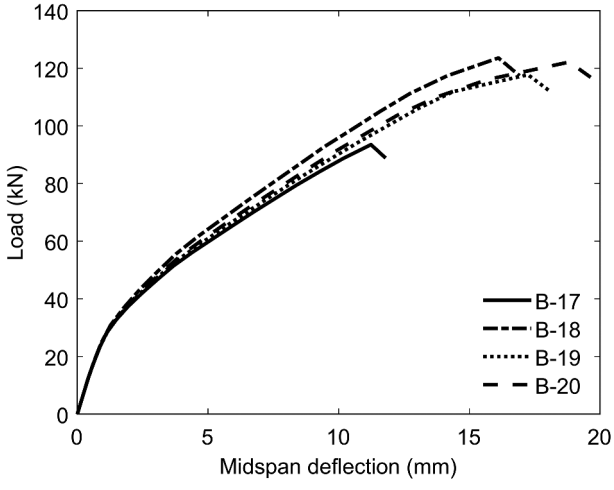

Figure 9. Influence of different FRP materials on beams' performance.

Table 6. Effect of different FRP materials.

Designation	FRP materials	P_u (kN)	Percentage increase in P_u over the control beam	δ_u (mm)
B-17	–	93.50	–	11.24
B-18	CFRP	123.58	32.17	16.11
B-19	GRFP	117.75	25.94	17.24
B-20	AFRP	122.17	30.66	18.82

Concrete compressive strength, f_c'=22.5 MPa
Steel reinforcement ratio, ρ = 1.4%
FRP rod diameter, d = 8 mm

RC beams using half-embedded CFRP, GFRP, and AFRP was 32.17%, 25.94%, and 30.66%, respectively, in comparison with the control and they were all observed to have the same response. This, therefore, means all types of the FRP rods used here can provide positive retrofitting effects for RC T-beams with half-embedded technique, while CFRP shows slightly better performance than the others based on the proposed analytical models. Meanwhile, it is important to note that these results depend on the properties of the FRP rods and there is a chance for difference based on the preference of the manufacturers.

5. Conclusions

Some models were developed in this research to analyze the flexural behavior of T-section RC beams strengthened in the negative moment region through the use of half-embedded FRP rods with the application of NSM technique. The models were validated through a comparison of two specimens' behavior and response with the findings of an experiment conducted by another researcher and a good relationship was established between the two studies. This was followed by the utilization of the validated models in the investigation of the effect of the size of the FRP rods, the compressive strength of the concrete, the ratio of steel reinforcement, and the type of the FRP on the flexural capacity of the strengthened beams using a design-oriented parametric study. The conclusions and observations from the research are, therefore, summarized as follows:

- The analytical models were observed to have the ability to imitate the specimens' flexural behavior with and without the application of half-embedded FRP rods.
- A direct relationship with a slight impact was established between FRP rod diameter and percentage increase in flexural capacity with the specimens strengthened using half-embedded FRP rods having 8, 10, and 12 mm diameter observed to have increased the flexural strength by 41.10%, 43.57%, and 46.50%, respectively.
- The compressive strength of the concrete was discovered to have a less substantial influence on the strengthened specimens' performance with the compressive strength at 25, 35, and 45 MPa causing an increment of 35.51%, 48.50%, and 57.25% respectively in the load-carrying capacity.
- A significant influence of the steel reinforcement ratio was observed in the RC T-beams strengthened using half-

embedded FRP rods in the negative moment region with the increment of 28.28%, 2.01%, and 2.34% recorded at 1.4, 2.1, and 2.95 reinforcement ratio, respectively.
- An increment in steel reinforcement ratio was found to reduce the percentage of the flexural strength for the half-embedded reinforced beam specimens and this further confirmed the effectiveness of this method in strengthening under-reinforced beam elements in the negative moment region.
- The properties and types of FRP were also found to have a substantial influence on the strengthened RC T-beams' performance with the CFRP rods discovered to have the highest value of flexural strength enhancement at 32.17% compared to the control specimen while the others including GFRP and AFRP rods had 25.94% and 30.66%, respectively.
- Since the developed analytical model did not take FRP sheets into consideration, the results reported herein should be considered in the light of some limitations that should be addressed in future research.

Nomenclature

ACI
American concrete institute

AFRP
Aramid fiber reinforced polymer

CFRP
Carbon fiber reinforced polymer

E_s
elastic modulus of steel

E_{sh}
strain hardening modulus of steel

f_c
compressive stress of concrete at a particular strain value

f_c'
compressive strength of concrete

FRP
fiber-reinforced polymer

f_s
stress of steel

f_t
tensile strength of concrete

f_u
ultimate strength of steel

f_y
yield strength of steel

GFRP
glass fiber reinforced polymer

k
factor of loss in post-peak for high-strength concrete

LVDT
Linear variable differential transformer

MCFT
Modified compression field theory

n
curve fit parameter

NMSE
Normalized mean square error

NSM
Near-surface mounted

P
strain-hardening parameter

P_u
ultimate load

$P_{u\text{-}An}$
ultimate load of analytical result

$P_{u\text{-}Exp}$
ultimate load of experimental result

R2K
Response-2000

RC
Reinforced concrete

δ_u
mid-span deflection at the ultimate load

ε_c
particular strain value of concrete

ε_{co}
strain at peak compressive strength

ε_s
strain of steel

ε_{sh}
initial strain at the beginning of strain hardening

ε_u
ultimate strain of steel

ε_y
yield strain of steel

ρ
steel reinforcement ratio

Acknowledgments

The first author acknowledges the support of the Ministry of Education, Taiwan (R.O.C) through the provision of the Elite Scholarship as well as the support of the CTCI Foundation in the form of the Research Scholarship for International Graduate Students.

Disclosure statement

No potential conflict of interest was reported by the author(s).

Funding

This research was funded by the Ministry of Science and Technology, Taiwan (R.O.C) under grant number MOST-108-2625-M-006-006.

References

ACI Committee 440. 2008. "*Guide for the Design and Construction of Externally Bonded FRP Systems for Strengthening Concrete Structures*." Report No. ACI 440.2R-08. Farmington Hills: American Concrete Institute.

Al-Khafaji, A., and H. Salim. 2020. "Flexural Strengthening of RC Continuous T-Beams Using CFRP." *Fibers* 8 (6): 41–58. doi:10.3390/fib8060041.

Bakis, C. E., L. C. Bank, V. L. Brown, E. Cosenza, J. F. Davalos, J. J. Lesko, A. Machida, S. H. Rizkalla, and T. C. Triantifillou. 2002. "Fibre-Reinforced Polymer Composites for Construction–State-of-the-Art Review." *Journal of Composites for Construction* 6 (2): 73–87. doi:10.1061/(ASCE)1090-0268(2002)6:2(73).

Bentz, E. C. 2000. "Sectional Analysis of Reinforced Concrete Members." PhD diss., Canada: University of Toronto.

Fayed, S., A. Basha, and A. Hamoda. 2019. "Shear Strengthening of RC Beams Using Aluminum Plates: An Experimental Work." *Construction and Building Materials* 221: 122–138. doi:10.1016/j.conbuildmat.2019.06.068.

Firmo, J. P., J. R. Correia, and L. A. Bisby. 2015. "Fire Behaviour of FRP-Strengthened Reinforced Concrete Structural Elements: A State-of-the-Art Review." *Composites Part B: Engineering* 80: 198–216. doi:10.1016/j.compositesb.2015.05.045.

Grace, N. F., G. A. Sayed, A. K. Soliman, and K. R. Saleh. 1999. "Strengthening Reinforced Concrete Beams Using Fiber Reinforced Polymer (FRP) Laminates." *ACI Structural Journal* 96 (5): 865–875. doi:10.14359/741.

Hollaway, L. C., and J.-G. Teng. 2008. *Strengthening and Rehabilitation of Civil Infrastructures Using Fibre-Reinforced Polymer (FRP) Composites*. Amsterdam: Elsevier.

Huang, Z. Y., T. S. Meng, N. Bagge, J. Nilimaa, and T. Blanksvärd. 2019. "Validation of a Numerical Method for Predicting Shear Deformation of Reinforced Concrete Beams." *Engineering Structures* 197 (109367–1–-109367–20): 109367. doi:10.1016/j.engstruct.2019.109367.

Jumaat, M. Z., M. M. Rahman, and M. A. Alam. 2010. "Flexural Strengthening of RC Continuous T Beam Using CFRP Laminate: A Review." *International Journal of the Physical Sciences* 5 (6): 619–625. doi:10.5897/IJPS.9000263.

Lam, N. J. W., and E. Lumantarna. 2011. "Force-Deformation Behaviour Modelling of Cracked Reinforced Concrete by EXCEL Spreadsheets." *Computers and Concrete* 8 (1): 43–57. doi:10.12989/cac.2011.8.1.043.

Lin, C.-T., Y.-H. Wu, W.-H. Chin, and M.-L. Lin. 2014. "Performance of CFRP-Strengthened RC Beams Subjected to Repeated Loads." *Journal of the Chinese Institute of Engineers* 37 (8): 1007–1017. doi:10.1080/02533839.2014.912778.

MacDonald, M. D., and A. J. J. Calder. 1982. "Bonded Steel Plating for Strengthening Concrete Structures." *International Journal of Adhesion and Adhesives* 2 (2): 119–127. doi:10.1016/0143-7496(82)90125-7.

Menegotto, M., and P. E. Pinto. 1973. "Method of Analysis for Cyclically Loaded Reinforced Concrete Plane Frames Including Changes in Geometry and Non-Elastic Behavior of Elements under Combined Normal Force and Bending." *Symposium on Resistance and Ultimate Deformability of Structures Acted on by Well Defined Repeated Loads*, Lisbon, Portugal, 12-14 September 1973. Zurich, Switzerland: International Association of Bridge and Structural Engineering (IABSE).

Metwally, I. M. 2012. "Evaluate the Capability and Accuracy of Response-2000 Program in Prediction of the Shear Capacities of Reinforced and Prestressed Concrete Members." *HBRC Journal* 8: 99–106. doi:10.1016/j.hbrcj.2012.09.005.

Nordin, H., and B. Täljsten. 2006. "Concrete Beams Strengthened with Prestressed near Surface Mounted CFRP." *Journal of Composites for Construction* 10 (1): 60–68. doi:10.1061/(ASCE)1090-0268(2006)10:1(60).

Panahi, M., and M. Izadinia. 2018. "A Parametric Study on the Flexural Strengthening of Reinforced Concrete Beams with near Surface Mounted FRP Bars." *Civil Engineering Journal* 4 (8): 1917–1929. doi:10.28991/cej-03091126.

Peled, A. 2007. "Confinement of Damaged and Non-Damaged Structural Concrete with FRP and TRC Sleeves." *Journal of Composites for Construction* 11 (5): 514–522. doi:10.1061/(ASCE)1090-0268(2007)11:5(514).

Popovics, S. 1973. "A Numerical Approach to the Complete Stress-Strain Curve of Concrete." *Cement and Concrete Research* 3 (5): 583–599. doi:10.1016/0008-8846(73)90096-3.

Porasz, A. 1989. "An Investigation of the Stress-Strain Characteristics of High Strength Concrete in Shear." M.A.Sc. thesis, Canada: University of Toronto.

Qeshta, I. M. I., P. Shafigh, and M. Z. Jumaat. 2016. "Research Progress on the Flexural Behaviour of Externally Bonded RC Beams." *Archives of Civil and Mechanical Engineering* 16 (4): 982–1003. doi:10.1016/j.acme.2016.07.002.

Raithby, K. D. 1982. "Strengthening of Concrete Bridge Decks with Epoxy-Bonded Steel Plates." *International Journal of Adhesion and Adhesives* 2 (2): 115–118. doi:10.1016/0143-7496(82)90124-5.

Sapulete, C. A. 2018. "Experimental Study on the Effect of FRP Rods and Wrap as A Flexural Strengthening on the RC Beams." [In Indonesian.] Master thesis, Indonesia: Diponegoro University.

Seckin, M. 1981. "Hysteretic Behaviour of Cast-in-Place Exterior Beam-Column Sub-Assemblies." PhD dissertation., Canada: University of Toronto.

Suryanto, B., R. Morgan, and A. L. Han. 2016. "Predicting the Response of Shear-Critical Reinforced Concrete Beams Using Response-2000 and SNI 2847:2013." *Civil Engineering Dimension* 8 (1): 16–24. doi:10.9744/ced.18.1.16-24.

Vecchio, F. J., and M. P. Collins. 1986. "The Modified Compression-Field Theory for Reinforced Concrete Elements Subjected to Shear." *ACI Journal* 83 (2): 219–231.

Zhang, H. Y., J. Yan, V. Kodur, and L. Cao. 2019. "Mechanical Behavior of Concrete Beams Shear Strengthened with Textile Reinforced Geopolymer Mortar." *Engineering Structures* 196 (109348–1–109348–11). doi:10.1016/j.engstruct.2019.109348.